Developments in the Built Environment 14 (2023) 100151

Contents lists available at ScienceDirect

Developments in the Built Environment

journal homepage: www.sciencedirect.com/journal/developments-in-the-built-environment

Detection of wire breaks in prestressed concrete bridges by Acoustic Emission analysis

Stephan Matthias Pirskawetz [a,*], Sebastian Schmidt [b]

[a] Bundesanstalt für Materialforschung und -prüfung (BAM), Unter den Eichen 87, 12205, Berlin, Germany
[b] Bilfinger Noell GmbH, Alfred-Nobel-Str. 20, 97080, Würzburg, Germany

ARTICLE INFO

Keywords:
Acoustic emission monitoring
Structural health monitoring (SHM)
Prestressed concrete bridge
Stress corrosion cracking
Wire break
Destructive testing
Nondestructive testing
Real scale test

ABSTRACT

The durability of prestressed concrete structures built between the 1950s and 1980s is becoming a growing problem. One reason is the sensitivity to stress corrosion cracking of the prestressing steel. Failure of prestressing wires can result in collapse of the entire structure without premature indication by transverse bending cracks or considerable deformation. The response of a structure to significant number of prestressing wire breaks was studied on a bridge in Brandenburg, Germany. Two thirds of the prestressing wires in concentrated tendons of two girders were cut before the bridge was demolished. Acoustic Emission Analysis was used to detect the wire breaks. Thus, the number of wire breaks was correlated with results of other measurement techniques, in particular strain measurements on the girders. In preparation of the measurements, the acoustic properties of the bridge were determined and the suitability of Schmidt hammer impacts as an acoustic reference source was validated.

1. Introduction

The development of prestressed concrete structures started in the early 20th century (Sanabra-Loewe and Capellà-Llovera, 2014). A milestone in this development was set by Eugène Freyssinet, a French engineer who applied for a patent to produce precast elements and a process of applying compression by pre-tension and bonded wires in 1928. The first prestressed concrete bridge with bonded tendons was built in 1936 in Oued-Fodda, Algeria. The first European bridge based on this system was built in 1938 in Oelde, Germany. It was in use until 2012 and is now a protected monument, relocated on a parking place near Beckum. The new technology became popular worldwide and different designs like slab bridges, slab and girder bridges or box girder bridges, construction processes like incremental launching or cantilever construction and prestressing methods like the Baur-Leonhardt method were developed, patented, and realized in the following decades. The Armet Bridge (1946) across the Marne River, France, was the first major bridge built in precast prestressed segmental construction (Billington, 1976). In India, as an example for Asia, the first prestressed concrete bridges, the Assam railway link bridges, were built in 1948 (Heggade, 2015). Built in 1950, the Walnut Lane Bridge in Philadelphia was the first prestressed concrete bridge in the United States (Billington, 1976).

In 2021 nearly 69% of the bridge deck areas in the German federal road network is made of prestressed concrete (Federal Highway Research Institute Germany (bast), 2021). As a consequence of destructions during World War II and the expansion of the road network in the post-war era economic boom, around 30% of the today's bridge area have been built in the 1950s–1970s (Federal Highway Research Institute Germany (bast), 2021). This era is characterized by slender, elegant, and sometimes courageous constructions. Even if most of the bridges are still in good condition, lack of experience of the engineers at the time confronts us with severe problems today, like corrosion of the tendons, fatigue of the tendons and wide cracks in the concrete. Causes of the different problems are insufficient prestresses, insufficient grouting, incomplete load assumptions (temperature differences ignored), unforeseen traffic loads, not enough unstressed reinforcement, inadequate design of coupling joints and stress corrosion cracking (SCC). Especially SCC can result in rupture of the prestressing wires and hence in a sudden failure of the structure without prior indication by concrete cracking, remarkable deformations, or visible corrosion products (fib Bulletin No. 26, 2003). Failure of prestressing steel can mainly be attributed to hydrogen induced SCC. Chapter 1 of the fib Bulletin 15 (fib Bulletin No. 15, 2001) reports on the status of the durability of post tensioned tendons in the United Kingdom, Germany, France, the United States,

* Corresponding author.
E-mail addresses: stephan.pirskawetz@bam.de (S.M. Pirskawetz), sebastian.a.schmidt@bilfinger.com (S. Schmidt).

https://doi.org/10.1016/j.dibe.2023.100151
Received 21 December 2022; Received in revised form 21 March 2023; Accepted 23 March 2023
Available online 24 March 2023

Canada and Japan. Corrosion due to inadequate grouting, sealing and chloride ingress is cited as one of the main problems. SCC is reported from France and Germany. fib Bulletin 26 (fib Bulletin No. 26, 2003) reports on failures of concrete structures due to SCC. Most of these cases originate from Germany. Prestressing steel sensitive to SCC has been produced in West Germany until 1964 (Felten & Guillaume Carlswerke AG, Trademark "Neptun") and 1978 (Hütten-und Bergwerke Rheinhausen AG, Trade Mark "Sigma") and in East Germany until 1993 (Stahlwerke Hennigsdorf) (Lingemann, 2010).

It usually takes several years until a bridge under suspect for SCC and without sufficient and early indication of failure can be replaced. Closing of bridges often causes long detours and doesn't protect the traffic below the bridge. Emergency scaffolding may only be an addition or last resort, which is not always feasible due to e.g., constructive limitations or underpassing connections. For safety reasons a monitoring of these bridges regarding breaks of prestressing wires becomes necessary. Until now the only reliable monitoring technique for detection of wire rupture in prestressed concrete structures is Acoustic Emission (AE) Testing. First field tests were carried out in the beginning of the 2000s in the UK (Cullington et al., 1999), (Cullington et al., 2001) and Japan (Yuyama et al., 2007). Starting in 2004, the prestressed concrete bridge Ponte Moesa in Roveredo/Canton Graubünden (Switzerland) was monitored with a total of 16 AE sensors. The project was supervised by ETH Zurich. A following scientific project laid the foundation for the today's methods used for detection of prestressed wire rupture by AE (Fricker and Vogel, 2006), (Fricker, 2009).

At time AE has become an established method for structural health monitoring (SHM) for detection of wire breaks in prestressed concrete structures (Schmidt and Salg, 2020), (Sodeikat et al., 2019). It is estimated that 10 to 20 structures in Germany are equipped with AE systems. The number of AE sensors varies between 12 sensors for small structures and reaches up to 248 AE channels for large structures. Since AE can detect active wire breaks only during the operation of the monitoring, it is essential to evaluate the condition of the structure in advance. Electrochemical techniques as described in (RILEM TC 154-EMC, 2003) and remanent magnetism method (Scheel and Hillemeier, 1997) for detecting of broken wires can assist in determining the current condition of the structure. Other inspection methods are summarized and evaluated in (Matt and Taerwe, 2001).

A part of the energy released during wire rupture propagates as elastic wave through the structure. The dynamic deformations of the surface caused by these so-called AE waves can be detected by piezoelectric AE sensors. An AE system detects an AE signal (output of the AE sensor) as a "Hit" if the signal amplitude crosses a predefined threshold, and AE signal features like Arrival Time (time of first threshold crossing), Rise Time, (peak) Amplitude, and Energy are extracted and stored. The signal feature (peak) amplitude is usually quoted in dB_{AE}. It is defined by $dB_{AE} = 20 \log (U/U_r)$; where U is the signal voltage referred to the preamplifier input and $U_r = 1$ μV is the reference voltage. For Energy calculation the AE signal voltage is squared and integrated within the signal duration. Further terms used specifically in AE testing are listed and defined in (EN 1330-9, 2009). Fig. 1 shows an AE signal of a wire break recorded on the bridge "Altstadtbrücke Brandenburg" during the destructive tests. An analysis of signal features allows to identify wire breaks and to separate such signals from noise. Sources of AE noise on bridges can be traffic, strong electromagnetic interference (e.g., from a pantograph of a train) or active cracks in concrete. Since wire breaks stimulate acoustic emissions of high energies and amplitudes, these signal features usually are the most important features for the identification of wire breaks. The analysis of arrival times is also a powerful tool for filtering of noise signals. Based on the arrival times of an AE waves from one source at different sensors, the location of the source can be calculated. Although AEs from concrete cracking near a sensor can result in high amplitude AE signals, they cannot be detected by distant sensors. Traffic can generate locatable signals that occur in the same place repeatedly. This is often caused by large joints or (loose) gully covers and must be considered when evaluating the data. Traffic also can generate noise that moves across the structure. This type of noise can usually be localized by arrival sequence zone location (EN 1330-9, 2009) and makes it possible to estimate the speed of the causing vehicle. Electromagnetic interference can be filtered out by too short arrival time differences at different sensors and by extraordinary high frequencies.

Detailed information about AE testing in different research fields and examples for technical applications are given for instance in (Miller et al., 2005) and (Grosse et al., 2022).

2. Experiments on the bridge

2.1. The bridge „Altstadtbrücke" in Brandenburg an der Havel

The „Altstadtbrücke" Brandenburg/Havel was a part of the federal road network in Germany. With a length of 180 m and a width of 37 m the bridge crossed a road and railway tracks of a steel works and of a regional train. It was designed to carry a four-lane road, two bicycle paths, two sideways, and two tramway tracks including tram stations. A distributer road on the north side connected the federal road B1 to the bridge. Fig. 2 shows an aerial photo of the bridge before it was blasted.

The bridge was built in 1969 as a bonded post-tensioned concrete construction. Ten continuous box girders were sectioned into five fields and supported by four rows of pillars with span lengths between 16 m and 40 m. The height of the box girders was about 1.5 m and did not vary

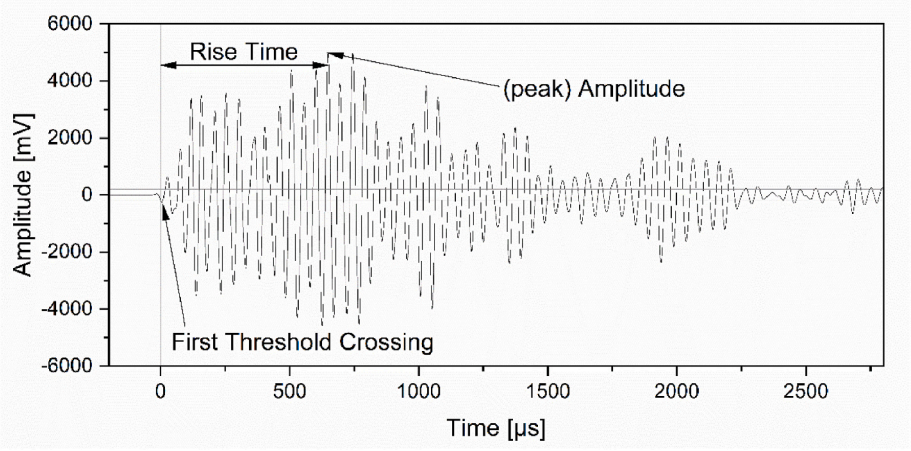

Fig. 1. AE signal of a wire break recorded on the "Altstadtbrücke Brandenburg".

Fig. 2. Aerial photo of the "Altstadtbrücke Brandenburg" shortly before it was blasted. Viewer looks south.

over the length and width of the bridge (see Fig. 3).

A characteristic of this bridge was the prestressing system. The prestressing wires in each girder were concentrated in one sheath with rectangular cross section. In the former German Democratic Republic (GDR) this method was known as "Spannblockverfahren" (TGL 173-33, 1967). It is comparable to the "Baur-Leonhardt"-technique, developed 1949 by F. Leonhardt and W. Baur in Stuttgart, West-Germany (Spannverfahren Baur Leonhardt, 1961), (Steinmann, 1954).

In the metal-sheet sheaths of the Altstadtbrücke the overall 392 wires per girder were arranged in 28 layers with 14 wires per layer. The oval ripped wires had a nominal cross section of 35 mm^2 and were spaced by sparer sheets. After mounting of the formwork and the reinforcement of the lower plate and the girder the full-length wires were laid one after the other into the sheaths. The sheaths than were sealed by welding a metal-sheet cover. After casting and hardening of the concrete in the whole structure the wire blocks were tensioned, and the sheaths were grouted. With this method it can't be avoided that the wires, which were made of Hennigsdorfer steel and therefore susceptible for SCC, were exposed to environmental moisture. In addition, the small wedges between the oval wires and the sparer sheets can form cavities, even if the quality of the grouting was good. Under these conditions the probability for an initial corrosion damage and incipient cracks is high.

A routine inspection in December 2019 revealed serious and fast-growing cracking in combination with separation of the concrete on the side of some girders following the location of the concentrated tendons. Based on experience from bridges with similar construction it was assumed that the crack pattern can be attributed to breakage of prestressing wires. Re-bonding of broken wires causes splitting-tensile forces in the tendon. The subsequent destructive tests confirmed that resulting cracks become visible at the concrete surface if around thirty percent of the wires in a tendon are broken (Steinbock et al., 2022). The expected crack pattern is sketched in Fig. 4.

The bridge was closed to traffic immediately and a detailed inspection of the whole construction was started. Taken samples of the prestressing wires showed a tensile strength reduced by one third compared to the nominal strength of the steel and the steel was embrittled considerably. Therefore, the bridge was kept closed and a monitoring system was installed to ensure the safety of the traffic below the bridge. The monitoring system included temperature, deformation, and inclination measurements as well as an AE system for detection of wire breaks. Even if there was no traffic load on the bridge, between June 2020 and May 2021 111 spontaneous wire breaks were detected and localized by AE measurements. The wire breaks were concentrated in certain parts of some girders whereas in other parts of the bridge nearly no wire breaks were localized. Breaking of wires was clearly related to the temperature gradient. Especially the deformations of the bridge during cold nights followed by sunny days triggered wire breaks.

Due to the massive and irreparable damage it was decided to

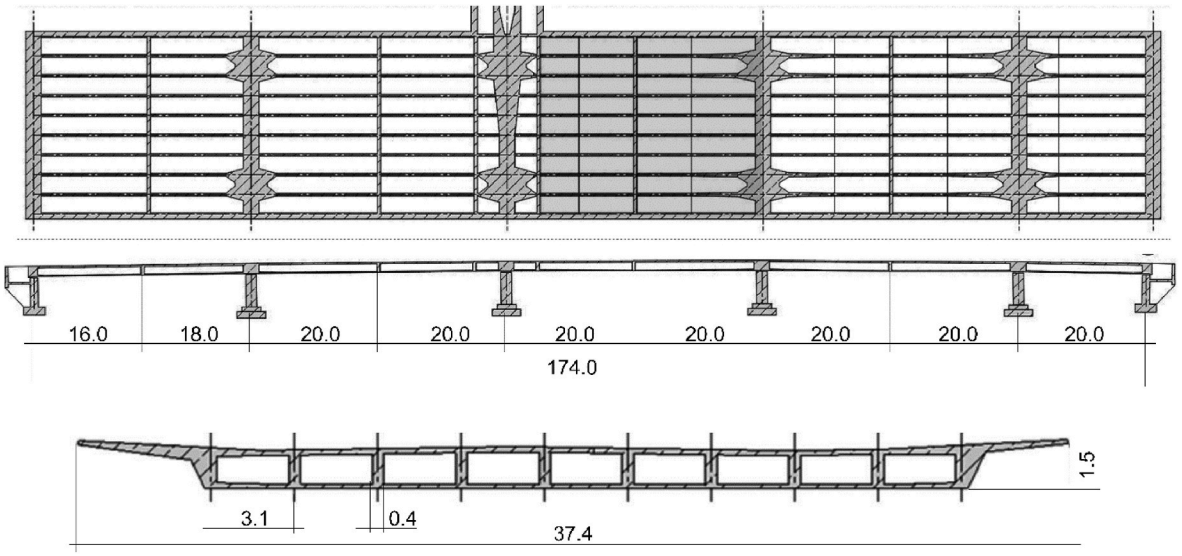

Fig. 3. Cross section of the "Altstadtbrücke Brandenburg". The test field is marked grey. Dimensions in m.

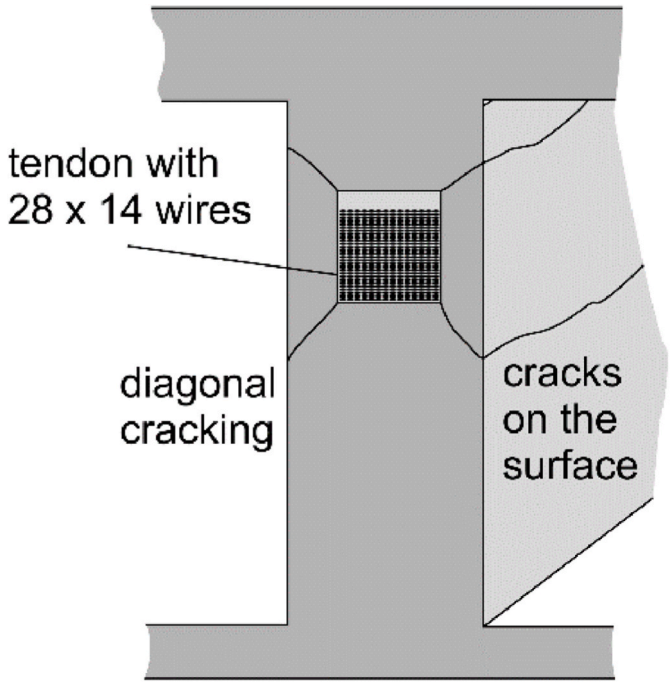

Fig. 4. Crack pattern expected around a concentrated tendon. Starting on the edges of the tendon cracks growth outwards in diagonal direction.

demolish the bridge as soon as possible. Before the bridge was blasted in May 2021, a team of researchers got the chance to carry out destructive tests on the bridge and to measure the reaction of the structure with various test methods like digital image correlation (DIC), fiber optic sensing, vibration analysis and AE analysis (Pirskawetz et al., 2022), (Bösche et al., 2021). The tests were planned by the University of Applied Science Dresden (HTW) and Technische Universität Dresden (TUD), organized by the Brandenburg Road Administration (LS Brandenburg) and financially supported by the German Federal Ministry for Digital and Transport (BMDV).

2.2. Experimental setup

To study the consequences of a substantial loss of prestress due to wire breaks the tendons of two girders were cut partially with a wire saw. The girders No. 4 and No. 8 were cut in Field 3 of the bridge which is marked grey in Fig. 3. The positions of the cuts are given in Fig. 5. Girder 4 was categorized as less damaged. During the period the AE monitoring was actively collecting data, only a few wire breaks were detected in Girder 4, Field 3 and the girder showed no significant concrete cracks in this area. In contrast, on Girder 8 the AE monitoring system detected a significant number of wire breaks, which resulted in severe cracks (regarding length and width) on the concrete surface of the girder. Girder 8 therefore was categorized as already severely damaged before it was cut in the destructive test.

To study the acoustic characteristics of wire breaks, wave propagation and attenuation, influence of sensor types and sensor positions the existing AE monitoring system was supplemented by 24 sensors on Girder 4 and Girder 8. The additional AE channels were synchronized to the existing monitoring system. The positions and types of selected sensors are listed in Table 1 and drafted in Fig. 5. Hot glue was used to acoustically couple the sensors directly onto the concrete. The sensors were additionally fixed with magnetic holders. For this purpose, metal sheets with openings for the sensors were screwed onto the concrete

Table 1
Positions and types of AE sensors in Field 3 of the bridge.

Sensor-No.	Type	Nominal Frequency Range [kHz]	Girder/Position [m]
24	VS30	25–80	4/1.4
34	VS30	25–80	4/20.8
77	VS30	25–80	4/34.3
78	VS30	25–80	4/31.3
79	VS12	7–58	4/31.3
80	VS30	25–80	4/28.6
81	VS45	20–450	4/18.6
82	VS150	100–450	4/18.6
83	VS30	25–80	4/18.6
85	VS30	25–80	4/13.2
90	VS30	25–80	4/7.2
98	VS30	25–80	8/13.4

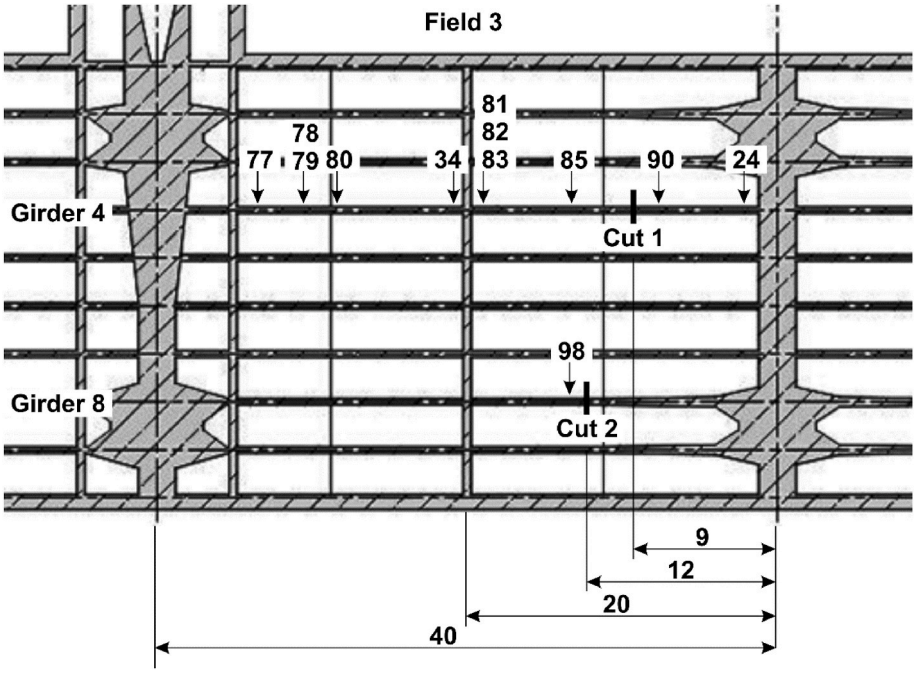

Fig. 5. Details of the test field with positions of cuts and selected sensors on the girders. Dimensions in m.

surface (Fig. 6). The quality of the acoustic coupling was tested by breaking pencil leads 50 mm away from the sensors (Hsu-Nielsen-Source 0.5 mm, 2H) according to ASTM E976 (ASTM E 976, 2015).

An AMSY 6 AE system with ASIP-2 signal processors and software AE Suite by Vallen Systeme GmbH was used to process, store, and analyze the AE signals. The bandpass filters of all channels were deactivated (bypass) and the detection thresholds of the channels were set individually, depending on the current local noise levels and sensor types. Compared to other applications of AE testing, wire ruptures of prestressing systems release signals of high energies and amplitudes. A signal amplification is needed for signal transmission only and the signals of the VS30 sensors therefore were amplified with 0 dB (factor 1). The maximum signal amplitude with this setup is 134 dB_{AE}.

Fig. 7 shows details of the sawing technique. A wire saw anchored to the bridge deck drove a diamond wire (Fig. 7 a)). The wire was guided via pulleys in the box girders (Fig. 7 b)) through bore holes in the bridge deck and in the girders (Fig. 7 c)). By sawing the sectional area of the single wires was reduced until the stress in the residual cross section reaches the tensile strength of the steel and the wire ruptured. It was intended to cut overall 252 wires of the tendons in 9 runs. With each sawing run around 28 wires (2 rows of 14 wires each) were cut. Breaks between the sawing runs were needed for a preliminary evaluation of the condition of the bridge based on the measured data. As drafted in Fig. 7 c) the diamond wire saw was slightly curved inside the concrete. Therefore, the prestressing wires were cut wire per wire starting from the outer wires. The AE system was used to count the number of breaking wires during sawing. This allowed to correlate wire breaks directly with the results of other measurements, in particular strain measurements using DIC. For DIC a high-contrast pattern of black on white paint was applied on the side of the girder in a field of 100 cm by 150 cm at a distance of 50 cm from the cut (Bösche et al., 2021). Digital correlation of successively acquired images of such patterns makes it possible to calculate deformations of the surface (Pan et al., 2009).

During the destructive tests, the AE monitoring of the whole structure was continued. It was agreed to interrupt the sawing if unexpected accumulation of wire breaks in other parts of the bridge were detected. The online analysis of the AEs was used additionally to count the wire breaks on the cutting site and to control the number of cut wires per sawing run.

3. Results and discussion

3.1. Acoustic characterization of the structure

AE analysis is a passive testing method whereby no energy is induced to the test object by the measurement system. A reference source for AE's is therefore needed for an acoustic characterization of the structure,

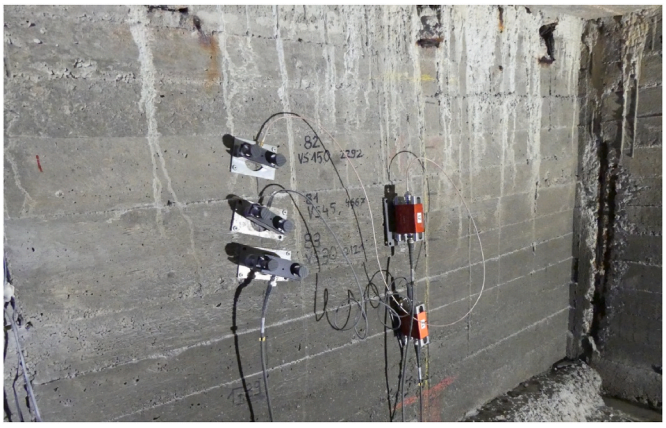

Fig. 6. Different types of AE sensors fixed with magnetic holders inside a box girder.

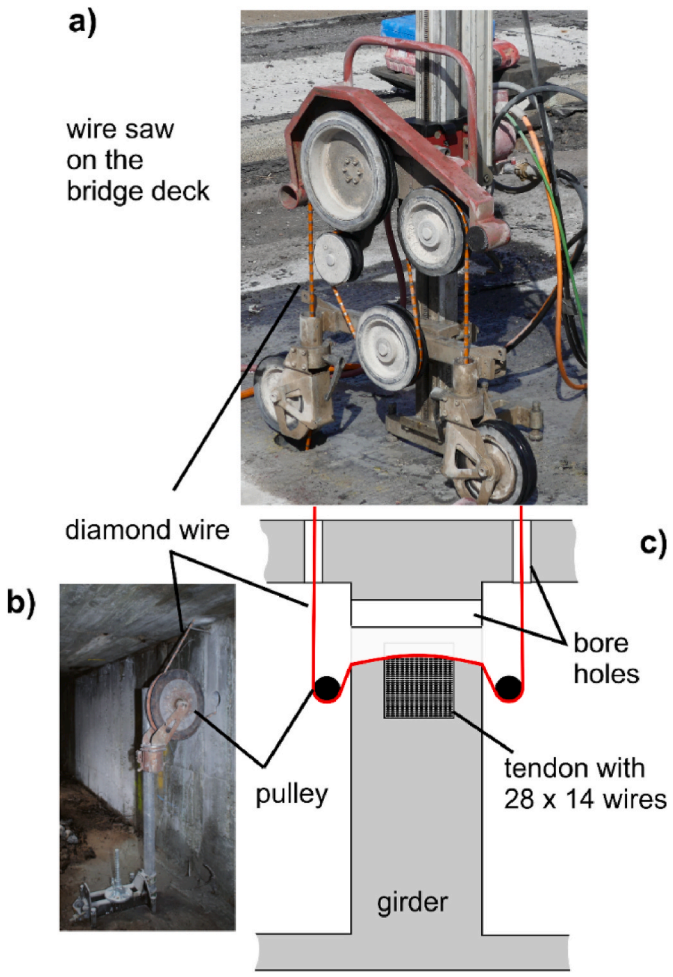

Fig. 7. Photo of the wire saw a), guidance of the diamond wire b) + c), and cross section of a girder c).

in particular to measure the signal attenuation in preparation of a monitoring, to check the function of the system and the uncertainty of source localization. If the signal amplitude of a source of interest (e.g., a crack or here in particular a wire break) is known, the k-value can be estimated. The k-value describes the amplitude ratio of the reference signal to the signal of interest. It is equal to the difference of the signal amplitudes quoted in dB_{AE}. The k-value given in dB_{AE} is negative if the amplitude of the reference signal is lower than the amplitude of the signal of interest. Based on the signal attenuation and the k-value, the maximum sensor distance for a reliable detection of all signals of interest can be determined. The procedure is described in (EN 14584, 2013). On steel structures like pressure vessels or large storage tanks the AE of a breaking pencil lead with hardness 2H, diameter 0.3 mm or 0.5 mm and length 3 mm (Hsu-Nielson-Source, according to ASTM E976 (ASTM E 976, 2015)) can serve as a reference source. In concrete the wave attenuation is much higher and such a Hsu-Nielsen-Source can be detected over a maximum range of one or 2 m. Additionally, the energy released by a wire break is expected to be much higher than the energy of a Hsu-Nielsen-Source.

Cullington et al. (1999), (Cullington et al., 2001) used the impact of a Schmidt hammer (Swiss hammer or rebound hammer) to stimulate artificial AE's in concrete structures. A Schmidt hammer impact has an energy of 2.2 Nm. It is highly reproducible and hence an appropriate reference source even if the energy transferred to the concrete and transmitted as an elastic wave depends on the concrete quality near the impact point.

After installation of the sensors a series of artificial AE's were

stimulated by impacts from a Schmidt hammer. The impact points were positioned approximately every 2 m on the sides at medium height of the Girders 4 and 8. The recorded AEs allow to analyze the acoustic characteristics of the structure.

The velocity of the elastic wave in a girder stimulated by the impact can be calculated based on the arrival time of the wave at two neighbored sensors. If the impact is located on the extension of the connecting line between the sensors the ultrasonic velocity can be calculated by dividing the sensor distance by the arrival time difference of the wave at the sensors. Table 2 shows the ultrasonic velocities estimated on different parts of Girder 4. The arrival times of the waves at the sensors were determined as the first crossing of the detection thresholds of the AE signals at the particular channels. A Schmidt hammer impact initially stimulates longitudinal waves perpendicular to the surface of the girder. Through mode conversion a mix of waveforms like longitudinal and surface waves propagates through the girder. For normal strength concrete, the velocity of the longitudinal wave is in the range of 4500 m/s, while the surface wave propagates at a velocity of approximately 3000 m/s. Depending on the distance between the sensor and the AE source, the onset of the low-amplitude longitudinal wave or the onset of the higher-amplitude surface wave is detected. The apparent AE velocities (EN 1330-9, 2009) therefore scatter in that range. Since there was no traffic on the bridge, the noise level was low and hence the detection threshold could be set comparatively low. In practical applications the detection threshold is usually set higher than 80 dB_{AE}. The measured (apparent) ultrasonic velocities are therefore in a range of 3500 m/s.

An important acoustic characteristic of a structure to be monitored is the attenuation of the acoustic waves. In combination with the noise level the attenuation limits the detection range of a sensor. Acoustic wave attenuation in prestressed concrete depends on the geometry of the structure, the concrete quality, and on the wavelength. Aggregates in concrete for structures such as the bridge in Brandenburg can have a maximum grain size of 32 mm. The aggregates are bound by a cementitious matrix which has a lower acoustic impedance than the aggregates. The inhomogeneous structure of concrete in the scale below around 5 cm causes intensive scatter and therefore high attenuation of acoustic waves with a wavelength below 10 cm–15 cm. At an ultrasonic velocity of 4000 m/s this corresponds to frequencies higher than 40 kHz.

Fig. 8 shows the frequency spectra of a Schmidt hammer impact detected by a VS150 AE sensor in a distance of 0.3 m, 2.1 m, and 4.5 m. Even over the short distance of 0.3 m the eigenfrequency of the sensor around 150 kHz was not stimulated by the hammer impact. The source obviously doesn't stimulate frequencies higher than 90 kHz. Due to the described frequency dependent attenuation already from a distance of 3 m, frequencies above 50 kHz can no longer be detected.

The pronounced attenuation of acoustic waves with wavelengths below 10 cm in concrete results in different detection ranges of different types of AE sensors. The higher the sensitivity in the lower frequency range, the larger is the range of detection. Fig. 9 shows a comparison of attenuation measurements with different types of sensors. Since the

Table 2
Ultrasonic velocities estimated on different parts of the structure, Detection Threshold: 80 dB_{AE}.

Sensor Pair	Distance Source – first hit Sensor	Distance between Sensors	Amplitude first/second hit Sensor	Arrival Time Difference	Calculated Ultrasonic Velocity
80–78	0.2 m	2.71 m	134/126 dB_{AE}	0.6 ms	4500 m/s
78–77	1.2 m	2.99 m	134/120 dB_{AE}	0.8 ms	3600 m/s
90–85	0.2 m	5.90 m	134/101 dB_{AE}	1.9 ms	3100 m/s
85–83	0.1 m	5.40 m	134/117 dB_{AE}	1.3 ms	4000 m/s

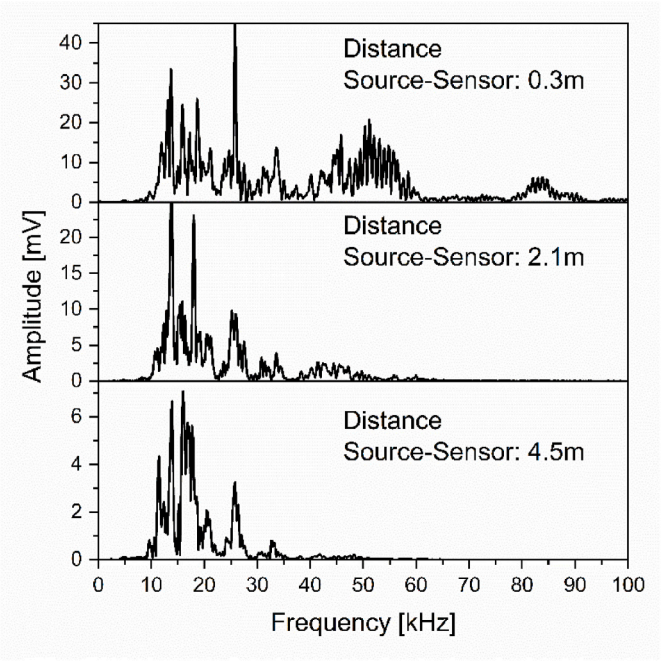

Fig. 8. Frequency spectrum of a Schmidt hammer impact detected by Sensor 82 (VS150) sensor in different distances to the source.

geometry of the structure is similar at the sensor locations it can be assumed that the geometric attenuation shows no significant differences. The influence of a geometric attenuation is therefore not considered in Figs. 9 and 12. The attenuation curves are calculated by a linear fit, excluding the overdriven measurements at short distances. As expected, the lowest attenuation was measured with the VS12. Considering the scatter of the measured amplitudes at different positions and sensors, the performance of VS30 and VS45 is comparable. This was not expected because of the high peak frequency of the VS45, but this sensor is also sensitive enough in the low frequency range. With knowledge of the attenuation, the detection range of a sensor at a certain position on the structure then can be estimated as the intersection with the evaluation threshold. It is recommended to set the evaluation threshold 3 dB_{AE} higher than the detection threshold. Therefore, the lower the detection threshold the longer the range of a sensor. The detection threshold is mainly determined by noise. It is practicable to allow a certain percentage of noise signals to cross the evaluation threshold and to remove these signals by subsequent filters in the data analysis. Otherwise, a detection threshold that is too low increases the filtering effort and the risk of misinterpretation of the detected signals.

Like the attenuation also the detected noise depends on the type of sensor. The main source of noise in bridges is the traffic on the bridge deck. Wheels rolling over (loose) gully covers, joints or small stones for instance stimulate low frequency AE's which are detected as noise. Low frequency sensors like the VS12 are therefore more sensitive to noise and a higher detection threshold can be necessary. The higher detection threshold reduces the detection range and thus can override the advantages of low frequency sensors.

Localization of AE events on the one hand is a powerful tool for filtering AE data. In the first step of the localization calculation AE signals detected at different neighbored sensors are grouped following certain time criteria. The arrival times of signals from the same AE source must be in the range of the time of flight of ultrasonic waves between the sensors. For a sensor distance of 10 m and an ultrasonic velocity of 3000 m/s for instance the timeframe is in the range of 4 ms. It is highly improbable that noise signals from independent sources arrive at two distant sensors in such a short timeframe. By excluding noise signals from stationary sources like loose gully covers or transverse

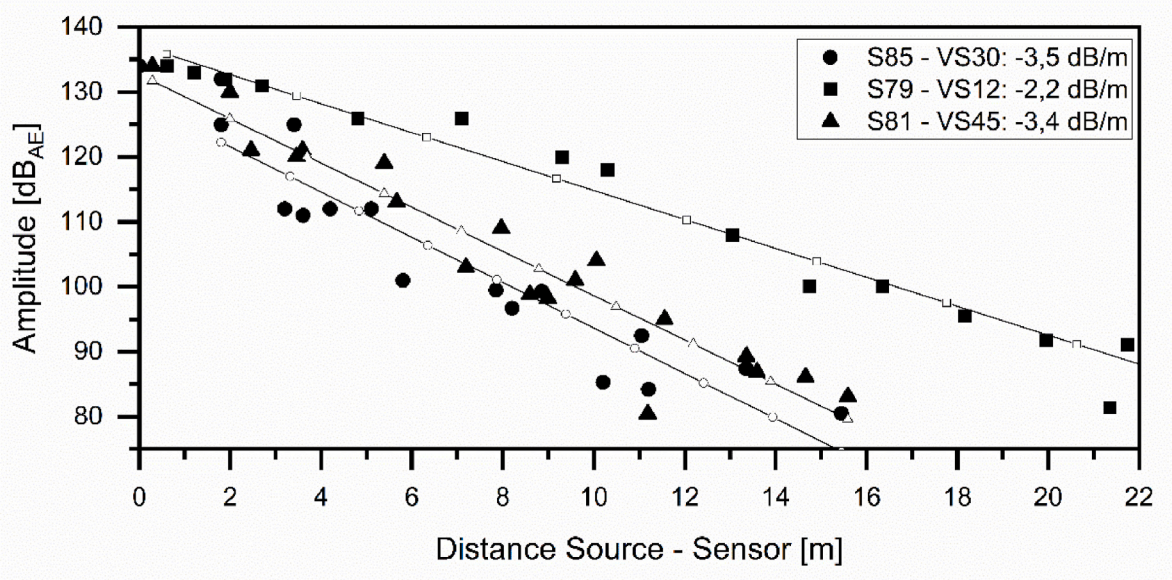

Fig. 9. Signal amplitudes of hammer impacts and attenuation curves as linear fits of the measured amplitudes for different types of sensors.

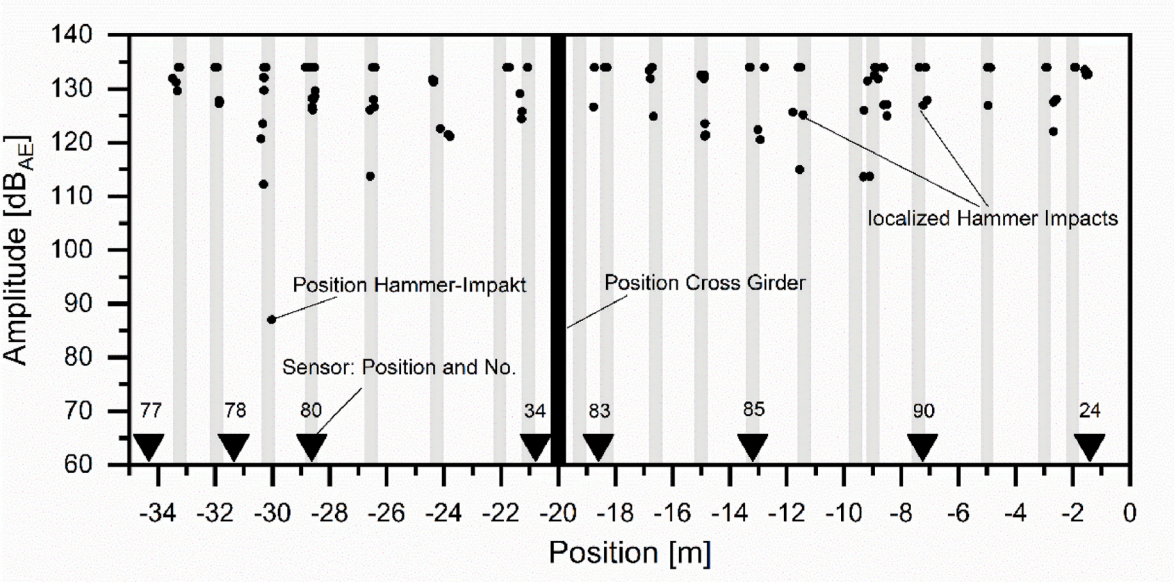

Fig. 10. Localization results for Schmidt hammer impacts on Girder 4.

joints the source of a localized event with a high amplitude at the first hit sensor is most likely a break of a prestressing wire.

On the other hand, localization of wire breaks is a valuable information for the responsible structural engineer. It supports an assessment of the damage evolution and a targeted inspection of the bridge. An accumulation of wire breaks can give hints to particularly vulnerable parts of the structure which than can be observed with special attention.

Fig. 10 shows localization results of hammer impacts on Girder 4 of the bridge in Brandenburg in comparison to the known positions of the sources, marked by the grey vertical lines. The width of the lines corresponds to approximately 50 cm. The localization error for most of the impacts in this test with a dense sensor network is smaller than ±50 cm. It is to point out, that the positioning of sensors is very irregular between the Sensors 80, 34 and 83 on Girder 4. This led to a higher location uncertainty in localization results between the Sensors 80 and 34. To avoid this effect, a variation of the sensor distance should be limited to a smaller than the presented factor. For practical applications a localization error of around 10% of the span with of a girder seems acceptable. For the Altstadtbrücke Brandenburg this corresponds to a location uncertainty of 4 m. In most applications the detection range of the sensors requires sensor distances which result in location errors below ±1 m.

3.2. Wire breaks

An important goal of the project was to assign the damage pattern of horizontal cracks in the concrete along the concentrated tendons to breaking of the prestressing wires. The development of such cracks during sawing could be visualized with DIC. Based on the DIC, the total crack width over the height of Girder 4 along a vertical line approximately 1 m from the cut. Fig. 11 shows the correlation between the measured deformation and the number of wire breaks detected with AE. Since the individual measurements points of the two techniques were not simultaneous, the respective time series were interpolated to

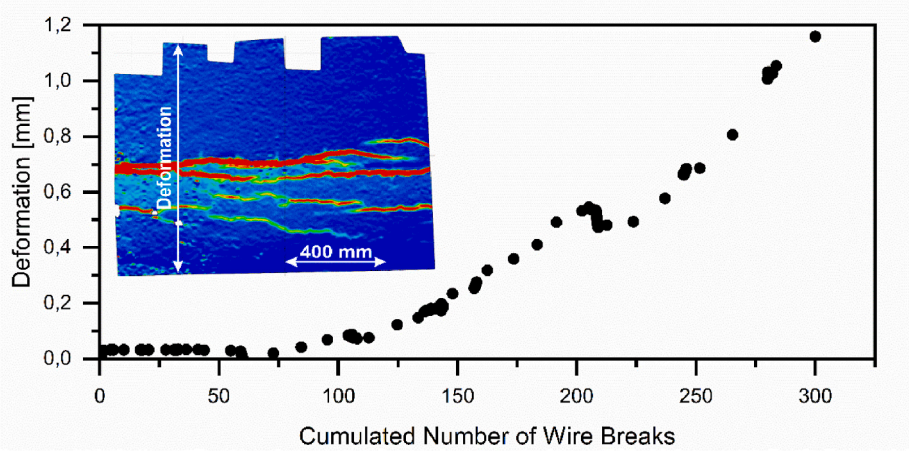

Fig. 11. Correlation between the Number of detected wire breaks and the vertical deformations measured with DIC about 1 m next to the cut on Girder 4. The graph inside the diagram shows the crack pattern visualized by DIC on the side of the girder after cutting. DIC data provided by (Steinbock and Bösche, 2021).

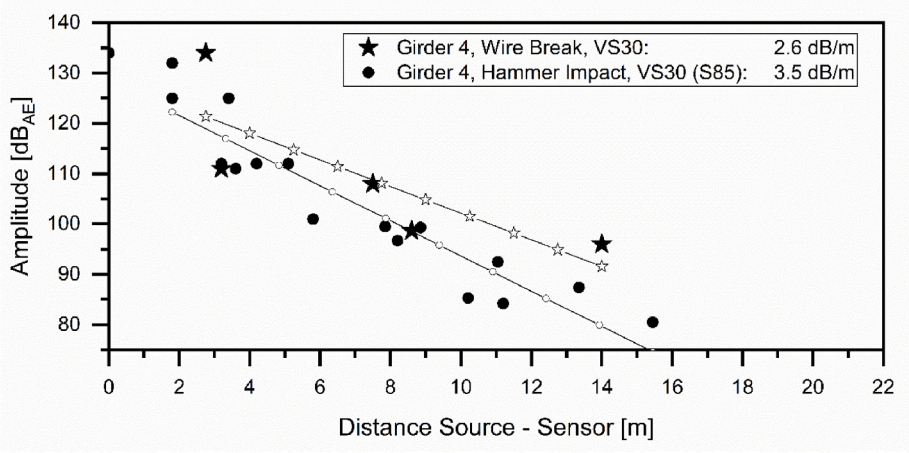

Fig. 12. Signal amplitudes of wire breaks and hammer impacts and attenuation curves as linear fits of the measured amplitudes.

equidistant points in time. Before the destructive test Girder 4 showed no significant cracks in concrete or separation of concrete along the concentrated tendons. According to Fig. 11 cracking on the concrete surface started after about 125 wires were cut. This is about one third of the total numbers of wires in the tendon. After the first crack formation, the relationship between wire breaks and crack growth is almost linear. The decrease in total crack width after 200 wire breaks occurred during a night break and can probably be attributed to temperature changes. After the test, the crack pattern on the side of the girder corresponded to the expected pattern as sketched in Fig. 4. The appearance of such cracks depends on details of the construction, such as the number and cross section of the wires, quality of grouting and thickness of the concrete cover. However, such cracks are in any case an indicator of serious damage to the tendon, so that detailed inspections should be initiated immediately and securing measures considered.

By analyzing the signals at different sensors, the attenuation of a wave stimulated by a wire rupture can be estimated. Fig. 12 shows the attenuation curve measured by VS30 sensors at different positions compared to Schmidt hammer impacts. In general, the amplitudes of the wire rupture signals are higher than the hammer impacts and the attenuation is lower. The lower attenuation may be explained by direction of the impact. A Schmidt hammer impact stimulates a displacement perpendicular to the surface whereas a wire break stimulates a material displacement inside the tendon in direction of the girder.

The main reason for the higher amplitudes of wire rupture signals is the higher energy released during rupture compared to a hammer impact. The energy E_{rel} released by a wire rupture can be estimated as follows.

$$E_{rel} = \sigma^2 / E * A * 0{,}5 * (l_{ptR} + l_{ptL})$$

For the bridge in Brandenburg the Young's modulus E of the prestressing wires is known (Bösche et al., 2021). The existing tension σ and the cross-section A of the wires were measured by taking samples (Bösche et al., 2021). The transmission lengths l_{ptR} and l_{ptL} on the left side and on the right side of the rupture until the wire after rupture is fully re-bonded to the surrounding grout or concrete depends on concrete quality, concrete cover, geometry and surface of the wire and other factors. It has not been measured and can only be roughly estimated regarding (EN 1992-1-1, 1992) and the results of Kommer (2008) and Ullner (2007). No studies describing the special situation in concentrated tendons have been found in literature. The extent of the transmission length is the main source for the high uncertainty of the estimated energy released by a wire break. The data for the Altstadtbrücke Brandenburg are summarized in Table 3.

Taking into account the significant uncertainty the energy released by a wire break should be 7 to 80 times higher than the energy of a Schmidt hammer impact of 2.2 Nm. Fig. 13 shows a comparison of energies of AE signals of wire breaks in relation to hammer impacts in the same distance to the sensor 90 at Girder 4 and sensor 98 at Girder 8.

The lowest wire break energy was 0.8 times the energy of a hammer

Table 3
Estimation of released energies of wire breaks based on properties of the wires measured on samples of the bridge in Brandenburg (Matt and Taerwe, 2001).

Cross-section	Young's Modulus	Tension	Transmission Length	Calculated Released Energy
A [mm^2]	E [N/mm^2]	σ [N/mm^2]	$l_{ptR} = l_{ptL}$ [mm]	E_{rel} [Nm]
35	205 000	680–810	200–1000	16–170

impact. It was measured on Girder 8 and in total only 2% of the signals had an energy lower than the hammer impacts. On Girder 4 the lowest energy ratio wire break to hammer impact was 2.2. In general, the portion of low energy wire breaks is higher in Girder 8 than in Girder 4. This can possibly be attributed to the higher degree of damage of Girder 8 already before the destructive tests. The low energies here could be explained by low tensions in wires which were cut near preexisting ruptures.

Overall, most of the measured energies are at the lower end of the estimated range. Assuming that Girder 4 was in a comparatively good condition and most wires were under a tension between 680 N/mm^2 and 810 N/mm^2, this leads to the conclusion that the transmission length in the compact, concentrated tendons is short. Local loss of prestress in single wires therefore leads to a stress redistribution into the surrounding wires. The growing local stress than increases the risk of additional wire breaks. This may explain the accumulation of wire breaks detected by AE monitoring in the one-year period before the destructive tests (Bösche et al., 2021).

The influence of the transmission length on the signal energy also must be considered if artificial wire breaks during sampling of wire samples are compared to hammer impacts. Depending on the sample length needed the wires must be uncovered on a certain length. During rupture therefore a longer part of the wire relaxes, and higher energy is released. This can lead to an overestimation of expected signal energies or amplitudes of spontaneous wire breaks. Nevertheless, the energies of spontaneous wire breaks will most likely be higher than those of the hammer impacts. On a logarithmic scale, Käding et al. (2022) found a linear relationship between signal amplitude and signal energy of wire breaks. By using a Schmidt hammer impact as reference source, the k-value than most likely will be negative. A wire break therefore can probably be detected over a greater distance than the Schmidt hammer reference source.

4. Summary

Before the prestressed concrete bridge "Altstadtbrücke" in Brandenburg/Havel, Germany, was blasted in May 2020 a consortium of researchers got the rare opportunity for destructive tests on the structure. In the real-scale test the concentrated tendons of two girders of the bridge were partially cut with a wire saw. The reaction of the superstructure of the bridge was measured with various nondestructive testing methods. The real-time AE data analysis performed during the tests was not only able to detect each wire cut but also to monitor the entire structure for spontaneous wire breaks and such which may have been caused by redistributed stress due to the severe damage induced by the wire saw. Regarding AE testing the results can be summarized as follows.

- By correlation of crack width and length measured with DIC and wire cuts counted by AE analysis it could be shown that cracking along girders in parallel to concentrated tendons is directly related to wire breaks.
- Impacts of a Schmidt hammer are well suited as reference signals. They can be used to measure the attenuation of acoustic waves in order to estimate the detection range of sensors at certain parts of the structure. The energy of Schmidt hammer impacts is usually lower than the energy of prestressed wire breaks.
- Due to the coarse meso-structure of the concrete the attenuation of acoustic waves with frequencies above 40 kHz is too high for detection of wire breaks over ranges longer than 2 m. For an efficient detection of wire breaks sensors with consistent sensitivity in the frequency range of 10–60 kHz can be recommended.
- The distance of two neighbored sensors along a girder should be lower than the detection range of the sensors. This ensures the detection of wire breaks by at least two sensors and allows a localization of the AE source. Localization is an efficient noise filter and a valuable information for structural engineers.

Currently AE analysis is the only reliable and economic monitoring method for detection of wire breaks in prestressed concrete structures. The installation and operation of a SHM system based on AE requires in-depth knowledge of the measurement technology, including the associated software and analysis procedures, combined with detailed knowledge of the structure. It must be pointed out that wire breaks can only be detected when the monitoring system is active. A detailed analysis of the structure's condition in advance is therefore essential for

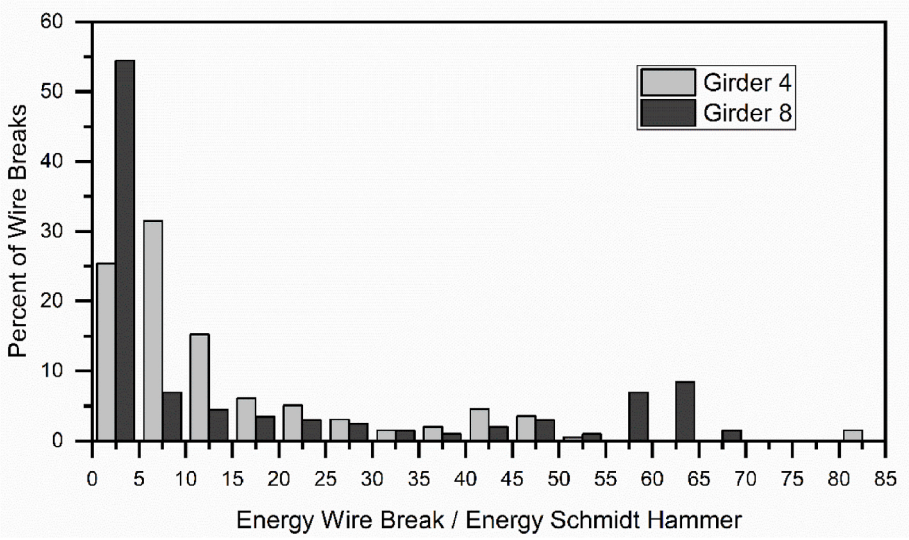

Fig. 13. Distribution of AE signal energies from wire breaks measured during sawing on the bridge "Altstadtbrücke Brandenbug".

assessing the damage evolution.

Declaration of competing interest

The authors declare that they have no known competing financial interests or personal relationships that could have appeared to influence the work reported in this paper.

Data availability

Data will be made available on request.

Acknowledgements

The authors thank the Brandenburg Road Administration (LS Brandenburg) for coordination and organization, the University of Applied Science Dresden (HTW) and Technische Universität Dresden (TUD) for technical planning of the tests and the German Federal Ministry for Digital and Transport (BMDV) for financial support of the project.

References

ASTM E 976, 2015. Standard Guide for Determining the Reproducibility of Acoustic Emission Sensor Response.

Billington, D.B., 1976. Historical perspective on prestressed concrete. PCI J. 21, 48–71. September-October 1976.

Bösche, T., Kaplan, F., Pirskawetz, S., Saloga, K., Steinbock, O., 2021. B1—Brücke Altstädter Bahnhof in Brandenburg an der Havel—Bauwerksuntersuchungen vor dem Rückbau. Landesbetrieb Straßenwesen Brandenburg. Website queried on. https://www.ls.brandenburg.de/sixcms/media.php/9/Brosch%C3%BCre_Bauwerksuntersuchungen%20B1%20%E2%80%93%20Br%C3%BCcke%20Altst%C3%A4dter%20Bahnhof%20in%20Brandenburg%20a.d.H..4172749.pdf. (Accessed 20 December 2022).

Cullington, D.W., MacNeil, D., Paulson, P., Elliott, J., 1999. Continuous acoustic monitoring of grouted post-tensioned concrete bridges. In: Conference Proceedings of International Structural Faults & Repair- 1999 8th International Conference (London, England).

Cullington, D.W., Paulson, P., Elliott, P., 2001. Continuous Acoustic Monitoring of Grouted Post-Tensioned Concrete Bridges. NDT&E International (Non Destructive Test & Evaluation) V34, N°2, March 2001, pp. 95–106.

EN 1330-9, 2009. Non-destructive Testing – Terminology – Part 9: Terms Used in Acoustic Emission Testing. Trilingual version.

EN 14584, 2013. Non-destructive Testing – Acoustic Emission Testing – Examination of Metallic Pressure Equipment during Proof Testing – Planar Location of AE Sources.

EN 1992-1-1, Eurocode 2: Design of Concrete Structures – Part 1-1: General Rules and Rules for Buildings.

Federal Highway Research Institute Germany (bast). Brückenstatistik 09/2021-internet. https://www.bast.de/DE/Statistik/Bruecken/Brueckenstatistik.pdf?_blob=publicationFile&v=17. (Accessed 20 December 2022). Website queried on.

fib Bulletin No. 15, 2001. Durability of Post-Tensioning Tendons. https://doi.org/10.35789/fib.BULL.0015.

fib Bulletin No. 26, 2003. Influence of Material and Processing on Stress Corrosion Cracking of Prestressing Steel – Case Studies.

Fricker, S., 2009. Schallemissionsanalyse zur Erfassung von Spanndrahtbrüchen bei Stahlbetonbrücken. Phd. Thesis. ETH Zürich. https://doi.org/10.3929/ethz-a-006027529.

Fricker, S., Vogel, T., 2006. Überwachung von Drahtbrüchen bei Stahlbetonbrücken (Monitoring of Wire-breaks of prestressed concrete bridges). Proceedings, Fachtagung Bauwerksdiagnose. Praktische Anwendung Zerstörungsfreier Prüfungen, Berlin, pp. 23–24. Feb. 2006.

Grosse, Ch U., Ohtsu, M., Aggelis, D.G., Shiotani, T. (Eds.), 2022. Acoustic Emission Testing. Springer International Publishing. https://doi.org/10.1007/978-3-030-67936-1.

Heggade, V.N., 2015. Segmental precast technology for multi-span bridges (production, transportation and launching). In: Multi-Span Large Bridges. CRC Press.

Käding, M., Schacht, G., Marx, S., 2022. Acoustic Emission analysis of a comprehensive database of wire breaks in prestressed concrete girders. Eng. Struct. 270 (2022), 114846 https://doi.org/10.1016/j.engstruct.2022.114846. S.

Kommer, B., 2008. Zur Verbundverankerung bei Vorspannung mit sofortigem Verbund in Hochleistungsbetonen, Phd. Thesis, Fakultät für Bauingenieurwesen der Rheinisch-Westfälischen Technischen Hochschule Aachen, 2008. https://d-nb.info/1000827437/34.

Lingemann, J., 2010. Zum Ankündigungsverhalten von älteren Brückenbauwerken bei Spannstahlausfällen infolge von Spannungsrisskorrosion, Phd. Thesis, Fakultät für Bauingenieur- und Vermessungswesen der Technischen Universität München.

Matt, P., 2001. Non-destructive evaluation and monitoring of post-tensioning tendons. In: Taerwe, L. (Ed.), Fib Bulletin 15, Durability of Post-tensioning Tendons, pp. 103–108.

R. K. Miller, E. Hill (technical editors), P.O. Moore (editor), 2005. Nondestructive Testing Handbook, Volume 6, Acoustic Emission Testing. Third Edition, Published by the American Society for Nondestructive Testing.

Pan, B., Qian, K., Xie, H., Asundi, A., 2009. Two-dimensional digital image correlation for in-plane displacement and strain measurement: a review. Meas. Sci. Technol. 20 https://doi.org/10.1088/0957-0233/20/6/062001.

Pirskawetz, S., Steinbock, O., Hille, F., Schmidt, S., Hofmann, D., 2022. Erfahrungen aus dem Rückbau der Brücke am Altstädter Bahnhof in der Stadt Brandenburg Teil 2: schadensmonitoring bei zerstörenden Versuchen. Beton- Stahlbetonbau 117 (2022), 8. https://doi.org/10.1002/best.202200052. Heft.

RILEM TC 154-EMC, 2003. 'Electrochemical techniques for measuring metallic corrosion' – recommendations. In: Half-cell Potential Measurements – Potential Mapping on Reinforced Concrete Structures. Prepared by Elsener, B., Materials and Structures, vol. 36.

Sanabra-Loewe, M., Capellà-Llovera, J., 2014. The four ages of early prestressed concrete structures. PCI J. 59, 93–121. https://doi.org/10.15554/pcij.09012014.93.121.

Scheel, H., Hillemeier, B., 1997. Capacity of the remanent magnetism method to detect fractures of steel in tendons embedded in prestressed concrete. NDT&E International 30, 211–216.

Schmidt, S., Salg, D., 2020. Spannbetonbrücke durch Schall überwachen. Bauingenieur, pp. 20–24, 2020; September 2020.

Sodeikat, C., Groschup, R., Knab, F., Obermeier, P., 2019. Acoustic Emission in der Bauwerksüberwachung zur Feststellung von Spannstahlbrüchen. Beton-Stahlbetonbau 114 (10), 707–723, 2019.

Spannverfahren Baur Leonhardt, 1961. Spannverfahren „Baur-Leonhardt". V 6225. Geltungsdauer bis 31.12.1961.

Steinbock, O., Bösche, Th, 2021. DIC Data of the Tests at the Altstadtbrücke Brandenburg.

Steinbock, O., Bösche, T., Ebell, G., Kaplan, F., Marzahn, G., 2022. Erfahrungen aus dem Rückbau der Brücke am Altstädter Bahnhof in der Stadt Brandenburg Teil 1: untersuchung und Erkenntnisse zum Ankündigungsverhalten bei großformatigen Spannngliedern mit spannungsrisskorrosionsgefährdetem Spannstahl. Beton-Stahlbetonbau 117 (2022), 8. https://doi.org/10.1002/best.202200051. Heft.

Steinmann, G., 1954. Das Verfahren Baur-Leonhard und die Ausführung von Brücken in vorgespanntem Beton. Schweizerische Bauzeitung. https://doi.org/10.5169/SEALS-61286, 1954.

TGL 173-33, 1967. Spannblockverfahren – Spannglieder mit Nennspannkraft 600 bis 1600 MP. Fachbereichsstandard. Ausgabe Juni 1967.

Ullner, R., 2007. Verbundverhalten von Litzenspanngliedern mit nachträglichem Verbund, Phd. Thesis, ETH Nr. 17424. ETH Zürich.

Yuyama, S., Yokoyama, K., Niitani, K., Ohtsu, M., Uomoto, T., 2007. Detection and evaluation of failures in high-strength tendon of prestressed concrete bridges by acoustic emission. Journal of Construction and Building Materials 21 (3), 491–500. March 2007, Fracture Acoustic Emission and NDE in Concrete (KIFA-4).